

## تجزئة صور شبكية العين للحصول على منطقة العصب البصري والأوعية الدموية

الدكتور مريم محمد ساعي\*

علي محمود ميا\*\*

(تاريخ الإيداع 8 / 7 / 2015. قُبِلَ للنشر في 14 / 1 / 2016)

### □ ملخص □

تقدم الدراسة طريقة جديدة لاقتطاع منطقة العصب البصري والأوعية الدموية من صور شبكية العين، تم استخدام صور من قاعدتي بيانات مختلفتين وتضمنت الصور المأخوذة حالات مختلفة مثل تغيرات الإضاءة واختلاف موقع العصب البصري في صورة الشبكية واختلاف تباين الصور وألوانها. تم التغلب على مشكلة الإضاءة من خلال اعتماد مرحلة معالجة مسبقة يتم فيها تصحيح إضاءة الصورة وفقاً للهستوغرام وتوزع السويات الرمادية فيها، بينما تم في المرحلة التالية استخدام العمليات المورفولوجية لترشيح الصورة الناتجة والحصول على المنطقة ذات الأهمية فيها، تلى ذلك عملية تحديد مركز العصب البصري ونصف قطره من خلال دراسة إحصائية للمنطقة الناتجة من المرحلة السابقة ثم اقتطاع العصب البصري، أما بالنسبة للأوعية الدموية فقد تم استخدام عمليات تصحيح الإضاءة ذاتها ثم الترشيح باستخدام المرشح الوسيط، وبإنجاز عملية الإغلاق والطرح وعمليات الفتح والتتحيف المورفولوجية تم التوصل إلى الصورة التي تتضمن منطقة الأوعية الدموية وتم بعد ذلك تعييبها وتحويلها للحصول على صورة الأوعية الدموية النهائية. أظهرت الدراسة في مرحلة اقتطاع العصب البصري أن 40 من أصل 50 صورة من قاعدة بيانات STARE قد تم تجزئتها بنجاح، في حين نجحت الخوارزمية على 84 من أصل 100 صورة من قاعدة بيانات DRIVE بمعدل اقتطاع 82.6%، بينما تم الحصول على جميع صور الأوعية الدموية منها بنسبة نجاح 100%. تمت مقارنة الدراسة مع الدراسات السابقة في المجال ذاته.

**الكلمات المفتاحية:** معالجة الصورة، تجزئة الصور الرقمية، شبكية العين، اقتطاع منطقة العصب البصري، التعرف على الأشخاص باستخدام شبكية العين، العمليات المورفولوجية.

\*أستاذ مساعد - قسم الحاسبات والتحكم الآلي - كلية الهندسة الميكانيكية والكهربائية - جامعة تشرين - اللاذقية - سورية.  
\*\*قائم بالأعمال - قسم هندسة الحاسبات والتحكم الآلي - كلية الهندسة الميكانيكية والكهربائية - جامعة تشرين - اللاذقية - سورية.

## Retina Segmentation to Obtain the Optic Nerve Area and Blood Vessels

Dr. Mariam M Saii\*  
Ali M Mayya\*\*

(Received 8 / 7 / 2015. Accepted 14 / 1 / 2016)

### □ ABSTRACT □

This paper proposes a new approach for the segmentation of the retina images to obtain the optic nerve and blood vessels regions. We used retinal images from DRIVE and STARE databases which include different situations like illumination variations, different optic nerve positions (left, right and center). Illumination problem has been solved by preprocessing stage including image histogram-based illumination correction. Next, some morphological operations were used to filter the preprocessed image to obtain the ROI region, then, the center and radius of optic nerve were determined, and the optic nerve region was extracted from the original image. In blood vessels segmentation, we applied the illumination correction and median filtering. Then the closing, subtraction and morphological operations were done to get the blood vessels image which was thresholded and thinned to get the final blood vessels image. At optic nerve segmentation, the study shows that 40 of 50 retinal images from STARE database were segmented correctly, and 84 of 100 from DRIVE database were extracted correctly which result in 82.66% segmentation rate, while the blood vessels were segmented correctly from all database images. The current study was compared with others at the same region.

**Keywords:** Image processing, Image segmentation, Retina image, Optic nerve segmentation, Retinal Human Recognition, Morphological operations.

---

\* Associate Professor, Department of computer and automatic control Engineering, Faculty of Mechanical and electrical Engineering, Tishreen University, Lattakia, Syria.

\*\* Academic Assistant,, Department of computer and automatic control Engineering, Faculty of Mechanical and electrical Engineering, Tishreen University, Lattakia, Syria.

## 1. Introduction

There are a lot of systems which discuss retinal images from the side of view of medical treatment or from side of retinal-based recognition systems. As a preprocessing step of that recognition and medical systems, the segmentation of optic nerve and blood vessels areas is required.

Image preprocessing steps play an important role in biometric and biomedical imaging-systems, due to its facilities especially in reducing past processing steps and enhancing algorithms results.

Lalonde2001 [1] try Hausdorff-based template matching algorithm on STARE and local retina image datasets, and he obtain 71.6% optic nerve segmentation rate for STARE images and 100% for local collected one.

Haar2005 [2] builds the Resolution pyramid using a simple Haar-based algorithm to segment the optic nerve. He used retinal images from STARE and local datasets, and got 70.4% and 89% segmentation rate for STARE and local databases.

R.ANAND, G.ARAVINTH BABU and K.DEEPA, V.LEKHA (2012) [3] applied Active Contour Model, Vector Flow model and Chan-Vese model for segmentation of optic nerve. The researchers didn't specify segmentation rate or database type.

Arumugam and Nivedha (2013) [4] used K-means clustering and Independent Component Analysis (ICA) to segment the optic nerve region from STARE and DRIVE databases, he got 94.3% (for STARE) and 100% (for DRIVE), but the datasets he used were small (40 for STARE & 53 for DRIVE).

OakarPhyo and AungSoeKhaing2014 [5] used Mathematical morphology methods such as closing, filling, morphological reconstruction and Otsu algorithm to segment the optic nerve; they used retinal images from websites and "Eye and ENT General Hospital (Mandalay) images. The system didn't mention any segmentation rate.

Josef Hájek, Martin Dražanský, and Radek Drozd 2013 [6] used bifurcations (points where a single vessel splits into two vessels) in retina. They applied their algorithm on STARE and DRIVE databases and got 64.26% (STARE) and 85% (DRIVE) for optic nerve segmentation, but they got 79.62% (STARE) and 92.9% (DRIVE) for blood vessels segmentation.

Some research at the same scope didn't treat the illumination variation, while the others didn't process the effect of degradation like different positions of optic nerve, different image sources, bad contrast, and color variations. This search is built to be robust against all of these conditions by applying a preprocessing correction step. The designed algorithm is fully automatic and don't need seed pixels unlike other research which depends on active shape contour and snakes and needs to determine the seed pixels. The proposed algorithms will work on retinal images of "JPG" format and uint8 type which has gray levels from 0 to 255.

## 2. Research Importance and Goals:

The research aims to segment the retinal images to obtain the optic nerve and the blood vessels region by using fast and efficient algorithm which works in presence of illumination variations and independent of the image nature like color or position. The research also aims to provide good segmentation accuracy and facilitate the diagnosis of retina's illness.

### 3. Methods and Tools:

The suggested algorithm consists of two operations:

- 1- Optic nerve extraction
- 2- Blood vessels extraction.

The optic nerve extraction consists of the following steps:

1. Read retinal image and transfer it into gray scale format and resize it to 600\*400.
2. Illumination correction when necessary: histogram-based and statistical-based techniques.
3. Image thresholding (threshold= 0.7).
4. Performing open morphological operation to illuminate outlier's points, and applying dilation to refill the gaps.
5. Detecting result area's center and radius to detect the optical nerve area.

The blood vessels extraction consists of the following steps:

1. Read retinal image and transfer into gray scale format.
2. Illumination correction when necessary: histogram-based and statistical-based techniques.
3. Median filtering of the corrected image
4. Perform closing morphological operation on the filtered image.
5. Subtract the filtered image from the closed one.
6. Brightening: Multiply the subtraction image by value 3.
7. Thresholding the multiplied image using threshold=0.05.
8. Remove outliers' points by means of opening.
9. Apply the thinning operation to get the blood vessels.

#### 3.1 Optic nerve extraction:

The following figure represents the block diagram of the proposed retinal segmentation system phase1 (the optic nerve extraction):

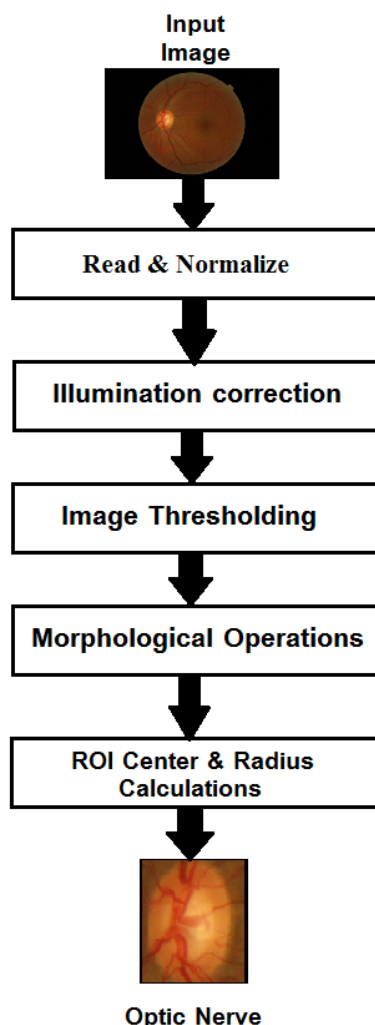


Figure 1. Block diagram of retinal segmentation system (phase1: the optic nerve extraction)

### 3.1.1 Illumination Correction:

Illumination problem is considered as common trouble that faces image processing. To avoid illumination variations problem, a new idea is suggested by using histogram of retina's image to detect the number of pixels which have a specific gray level. The idea is based on the fact that optic nerve area is the most brilliant area in the retina's image and have the biggest gray value, so it is normal to find a lot of 255-value pixels in retina's image (in uint8 image). From previous we can say this: "The retina's image which has a little number of 255 gray value (or almost 255) has low illumination level and should be adjusted" (modify its brightness) as follows:

$$S_i = \begin{cases} R_i * \exp(0.5) & \text{if num of high gray levels} < 10 \\ R_i & \text{otherwise} \end{cases} \quad (1)$$

Where  $R_i$  is the original gray level, and  $S_i$  is the output corrected gray level.

The reason of using the exponential function is the contrast stretching that it performs. Form figure (2) it can be noticed that the input gray scale (50-100) results in bigger output scale (82.5-164.8) which means higher brightness.

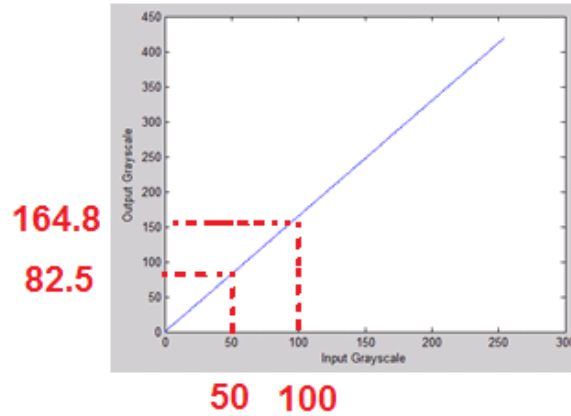


**Figure 2. Function of illumination correction process**

The previous plot is defined by the following equation:

$$S = r * \exp(0.5) \quad (2)$$

To deal with different types and resources of retinal images, the algorithm suggests resizing the input image to a fixed size [600-400], and then the illumination correction step is performed.

The following figure includes some examples of correction process on database's images:

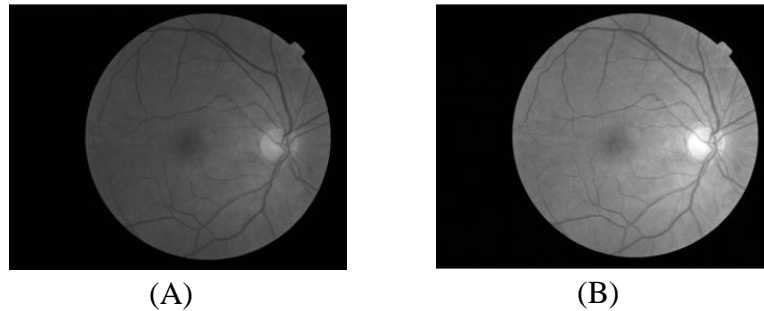


**Figure 3.illumination correction:(A) original image (B): corrected image**

It is important to say that illumination correction step doesn't increase the brightness of all pixels; otherwise, it affects the non-zero pixels only, and because the increasing process is done by multiplication, so the big gray level value will increase better than lower one and this will increase the contrast of the image.

### 3.1.2 Thresholding:

In this step the corrected image is converted into binary one using threshold value equal to 0.7 because the optic nerve image has high gray value (200-255).

The following figure shows the result of thresholding a corrected image with threshold  $T=0.7$  ( $0.7*255=178.5$ ) because the gray levels range of input image is [0-255].

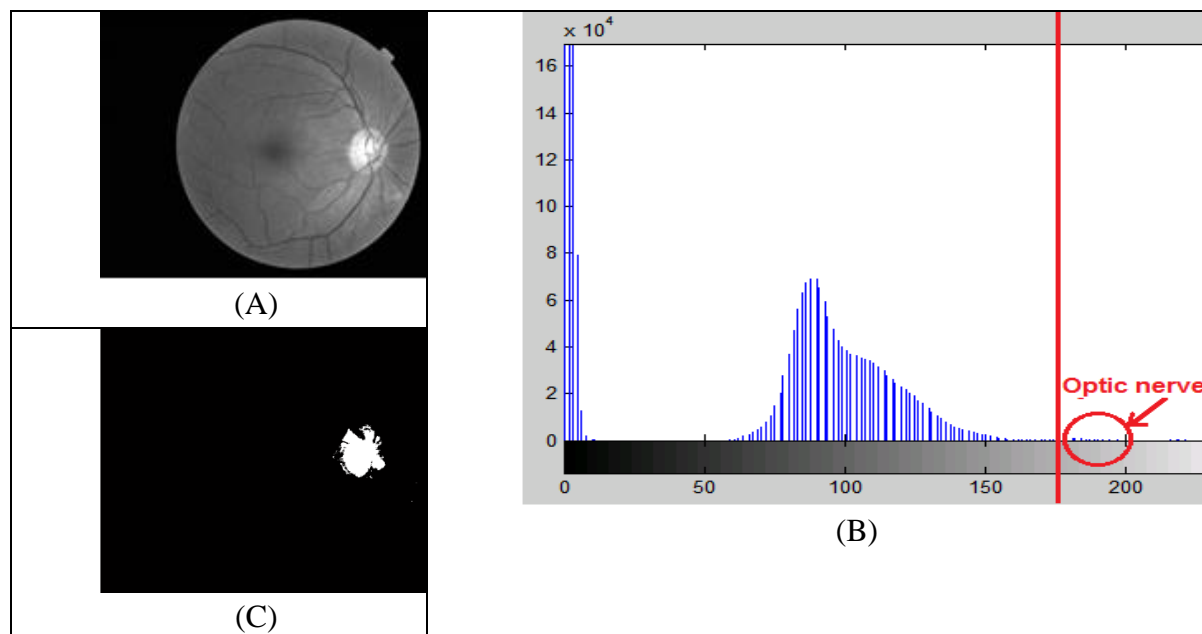


Figure 4. Thresholding the corrected image: (A) corrected image, (B) Histogram of corrected image (C) Thresholded image

### 3.1.3 Morphological Operations:

#### 3.1.3.1 Removing Outlier in thresholded Images:

An opening morphological operation is done to remove undesired points. This method removes the regions whose their area is lower than specific number (300) determined by experiment. The following equation illustrates the method:

$$Area_i = \begin{cases} 0 & \text{if } N(Area_i) < 300 \\ Area_i & \text{otherwise} \end{cases} \quad (3)$$

Where:  $Area_i$  is the area of region  $i$ ,  $N(Area_i)$  is the number of region's pixels.

#### 3.1.3.2 Filling Holes:

After removing the undesired points from thresholded image, it needs a filling-holes operation (Equation 4) to group the white region of interest (ROI) and fill the holes inside it, so we can calculate the ROI properties [7].

$$Image_{Filled} = (f \oplus h)(s) \cap (f^c \oplus h) \quad (4)$$

Where  $F$  is the original image,  $h$  is the structure element (3x3 squared ones matrix) and  $f^c$  is the complement of image ( $f$ ), and  $(f \oplus h)$  is the binary dilation process which is given as follows [7]:

$$(f \oplus h) = \{z | (\hat{h})_z \cap f \neq \emptyset\} \quad (5)$$

The dilation is the set of all displacements  $z$  such that  $\hat{h}$  and  $f$  overlap by at least one element. Figure 5 illustrates the filling holes process followed by dilation.

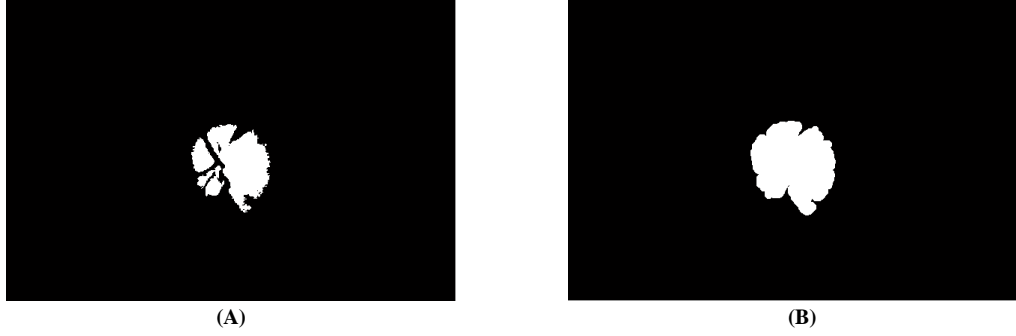


Figure 5. Filling Holes: (A), Opened image (B) Filled-Holes image

### 3.1.4 Detect and extract the optical nerve region:

The optical nerve (ROI) is detected by calculating the center [x,y] and radius of the grouped region obtained by the previous step. The proposed technique depends on the region properties to make these calculations. The radius is calculated as follows:

$$\text{Radius} = \frac{(\text{Major Axis} + \text{Minor Axis})}{2} \quad (6)$$

After detecting the center and radius of ROI, a circle whose center is [x,y] and radius is “Radius” calculated in the previous step is drawn, this circle is surrounding the ROI. The rectangle including the detected region is extracted as shown in figure 6.

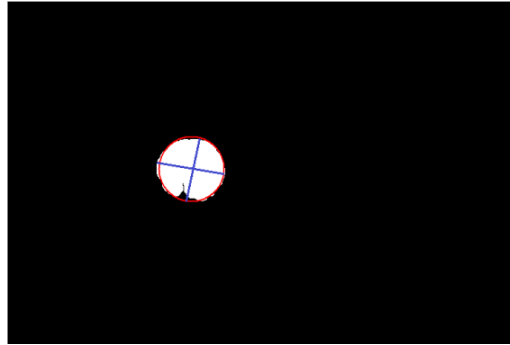


Figure 6. ROI detection

### 3.2 Blood Vessels extraction:

Figure 7 represents the block diagram of the proposed retinal segmentation system phase2 (the blood vessels extraction):



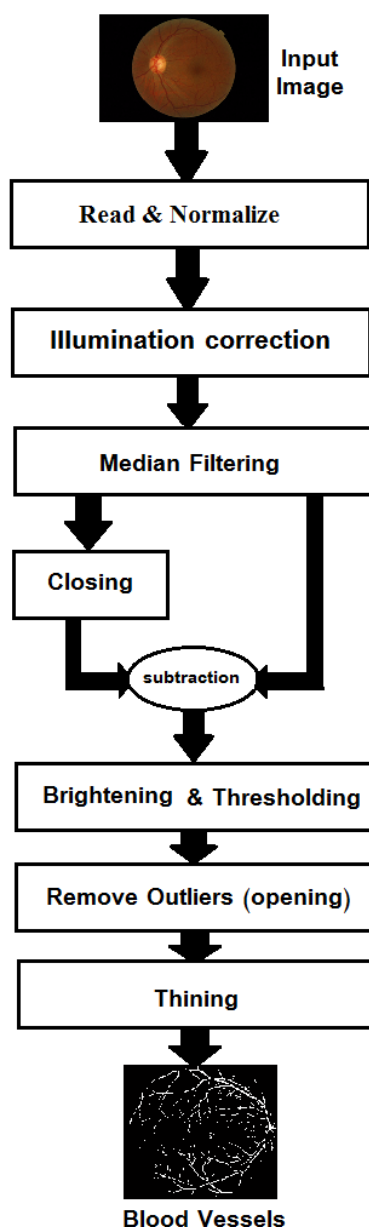


Figure 7. Block diagram of retinal segmentation system (phase2: the Blood Vessels extraction)

The first two steps are the same as the optic nerve extraction system so we go ahead with the next steps.

### 3.2.1 Median Filtering:

After the image is being transformed to gray format and its illumination has been corrected, we removed the very small lines in background which are considered as noise. The result cleared image is used as a mask image which will be subtracted from the closed one to get the blood vessels. The median filter we applied has a mask of size 25 pixels (5\*5). The filter is applied on each pixel of the image and its 24 surrounding pixels, where they are arranged exponentially and the middle pixel is chosen to replace the main pixel. Figure 8 includes an example of median filtering of retinal image.

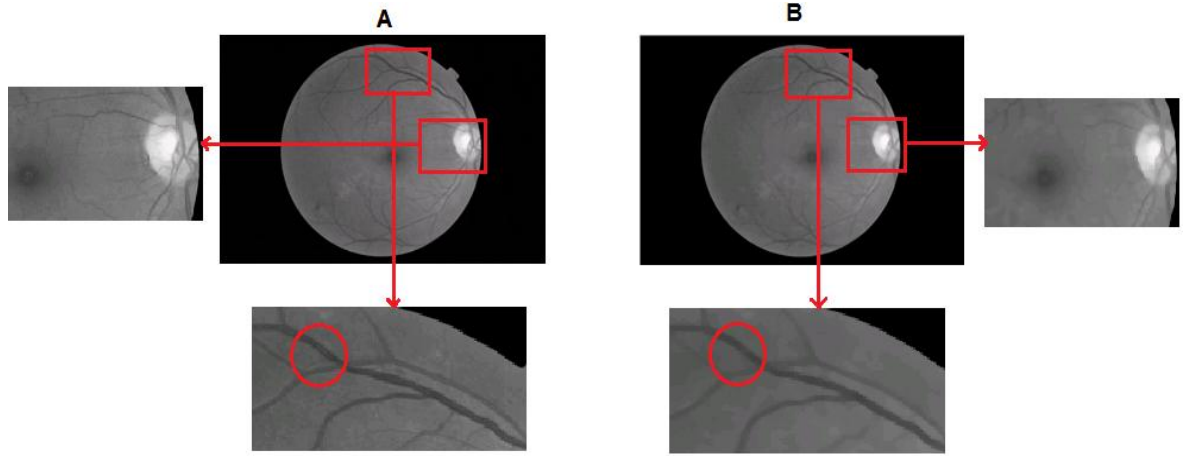


Figure 8. Median filtering: (A) the original image, (B): the median-filtered image

### 3.2.2 Obtain the blood vessels:

This step aims to get the blood vessels area by subtracting the mask image (median-filtered image) from the closed one.

First, we get the closed image by applying dilation process followed by erosion one.

Next, the filtered image will be subtracted from the closed one to obtain the blood vessels only by the following equation:

$$Image_{blood-vessels-1} = Image_{closed} - Image_{filtered} \quad (7)$$

The figure (9) illustrates the effect of applying closing and subtraction processes on the filtered image.

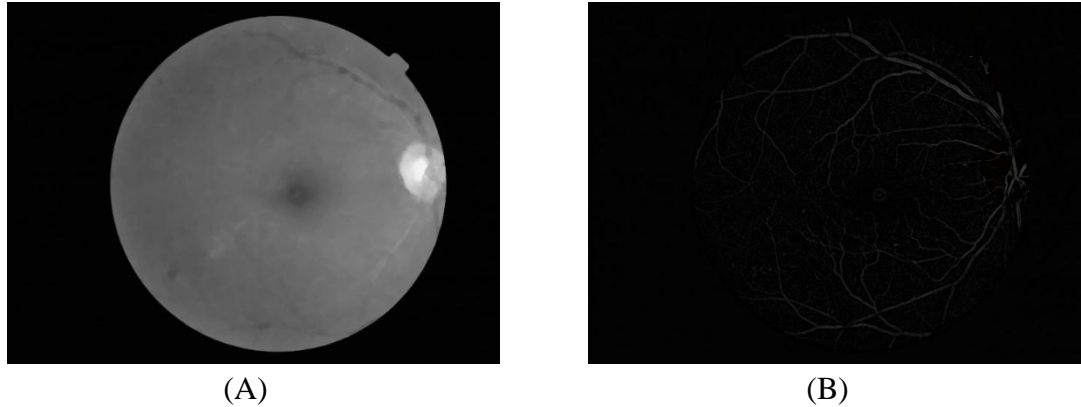


Figure 9. Obtain the Blood Vessels Steps: (A): Closed Image (B): Subtraction Result

### 3.2.3 Brightening and Thresholding:

After subtraction is performed, the result image includes the blood vessels only but the image still low in brightness. To correct that, we raise the intensity values of image three times higher than their real values.

$$Image_{blood-vessels-2} = 3 * Image_{blood-vessels-1} \quad (8)$$

After that, the image is transformed to the binary format by means of the following equation:

$$Image_{blood-vessels-noisy} = \begin{cases} 1 & \text{if } Image_{blood-vessels-2} \geq 0.05 \\ 0 & \text{otherwise} \end{cases} \quad (9)$$

Here is the result of applying brightening and thresholding processes on the subtraction output.

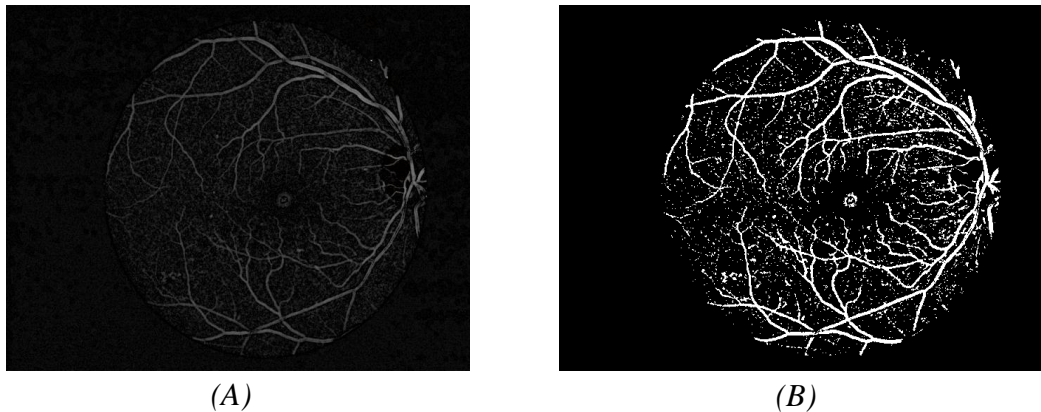


**Figure 10. Brightening and Thresholding: (A) Brightened image, (B): Thresholded image**

### 3.2.4 Remove Outlier's points:

The area-opening process removes the undesired small vessels and the other outlier's points whose area is less than 100 via the following equation:

$$Image_{blood-vessels-true} = \begin{cases} 1 & \text{if } Area(Image_{blood-vessels-noisy}) \geq 100 \\ 0 & \text{otherwise} \end{cases} \quad (10)$$

The following figure shows the result of opening the blood vessels image to get the final true blood vessels:

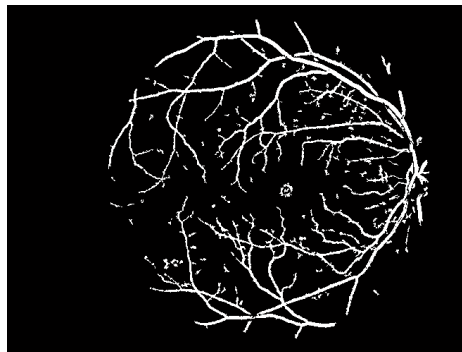


**Figure 11. Remove Outlier's points**

### 3.2.5 Thinning:

The final true blood vessels image is thicker than the original ones so the last step in system is the thinning process that is applied to obtain the final blood vessels image. The thinning is a morphological operation performed by multiple erosion steps by using the following structural elements:

-1 -1 -1	0 -1 -1	1 0 -1	1 1 0
0 1 0	1 1 -1	1 1 -1	1 1 -1
1 1 1	1 1 0	1 0 -1	0 -1 -1
1 1 1	0 1 1	-1 0 1	-1 -1 0
0 1 0	-1 1 1	-1 1 1	-1 1 1
-1 -1 -1	-1 -1 0	-1 0 1	0 1 1

Figure (12) illustrates the final thinned blood vessels images.

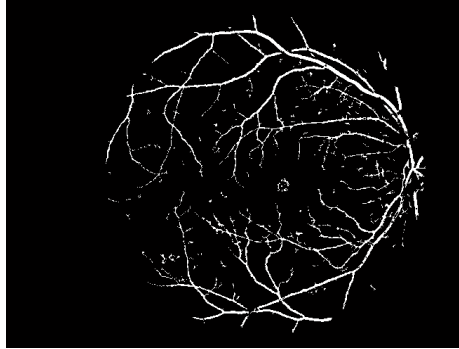


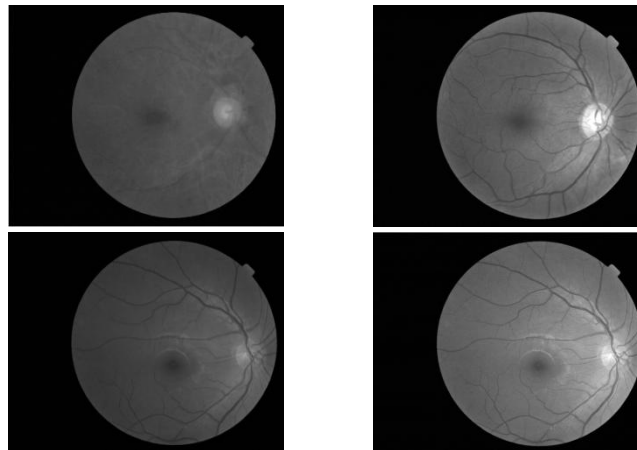
Figure 12. The Final Blood Vessels Image

## 4. Results and Discussion:

To test the proposed segmentation algorithm, DRIVE and STARE databases were used. We used 100 retinal images of size 2240\*1488 and “JPEG” format from the first database and 50 images of size 600\*400 and “JPEG” format from the second database. All images are of uint8 type whose gray levels are ranging between 0 and 255. The designed algorithm is written and tested in MATLAB 2010a.

### 4.1 Illumination correction tests:

Figure(13) shows some tests of the illumination correction step on the database images.



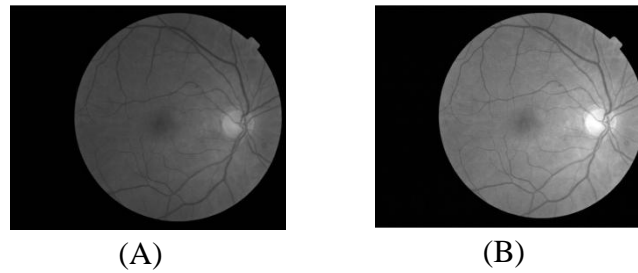
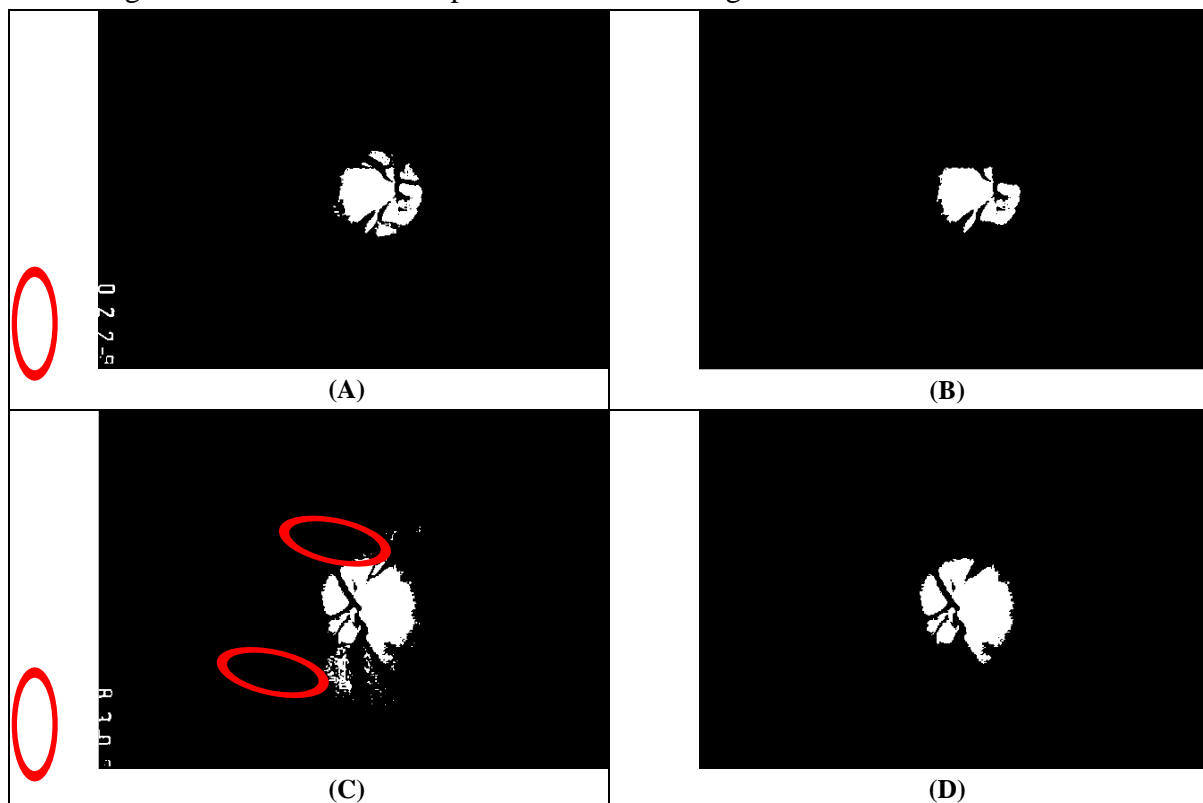


**Figure 13. examples of illumination correction step:  
(A) original images (B): corrected images**

It can be noticed that the optic nerve and blood vessels are not clear enough in images with low illumination i.e., the image' contrast is low. After applying the illumination correction step, the optic nerve and blood vessels become brighter and obvious. In the high-level illumination images, the correction process has no effects on the image.

#### 4.2 Remove outlier Tests:

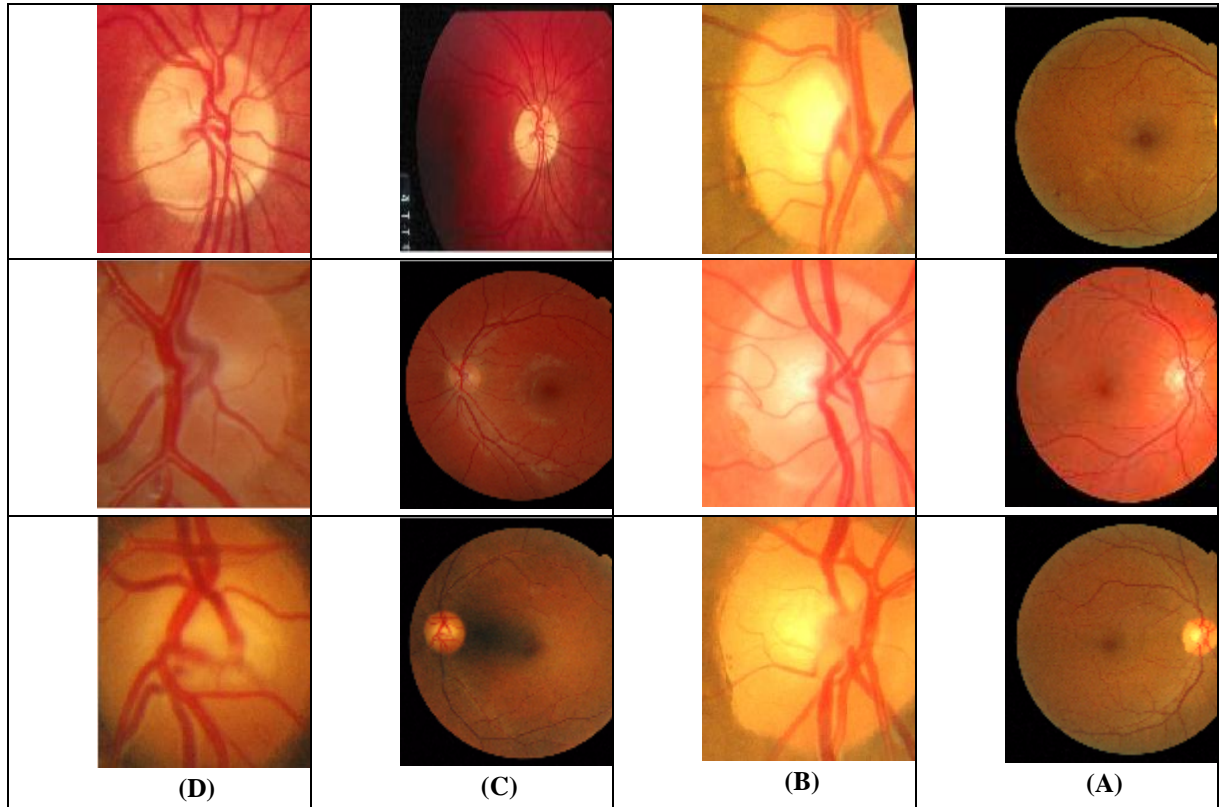
Figure 14 includes some experiments of removing outliers.



**Figure 14. Removing outliers: (A,C), Thresholded image (B,D) Opened image**

#### 4.3 Segmentation Tests:

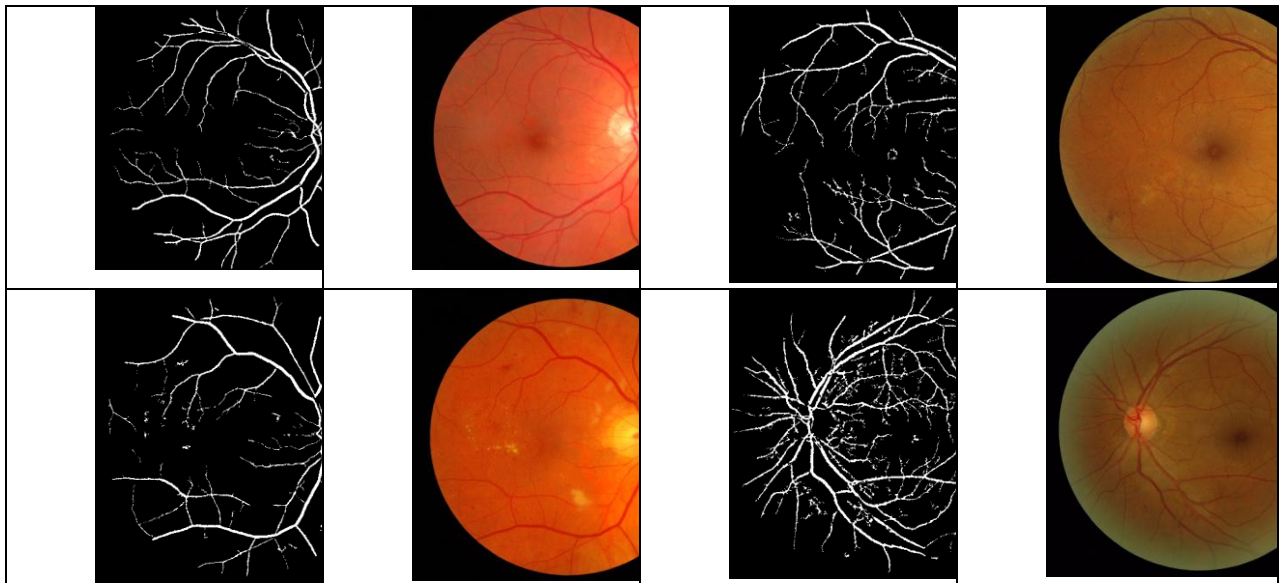
The figure 15 shows different conditions of retinal images in which the optic nerve is segmented correctly.



**Figure 15. Results of optic nerve segmentation from retinal images under different conditions**

**(A,C) Original Image, (B,D) Optic Nerve Region**

While the figure 16 shows different conditions of retinal images in which the blood vessels is segmented correctly.





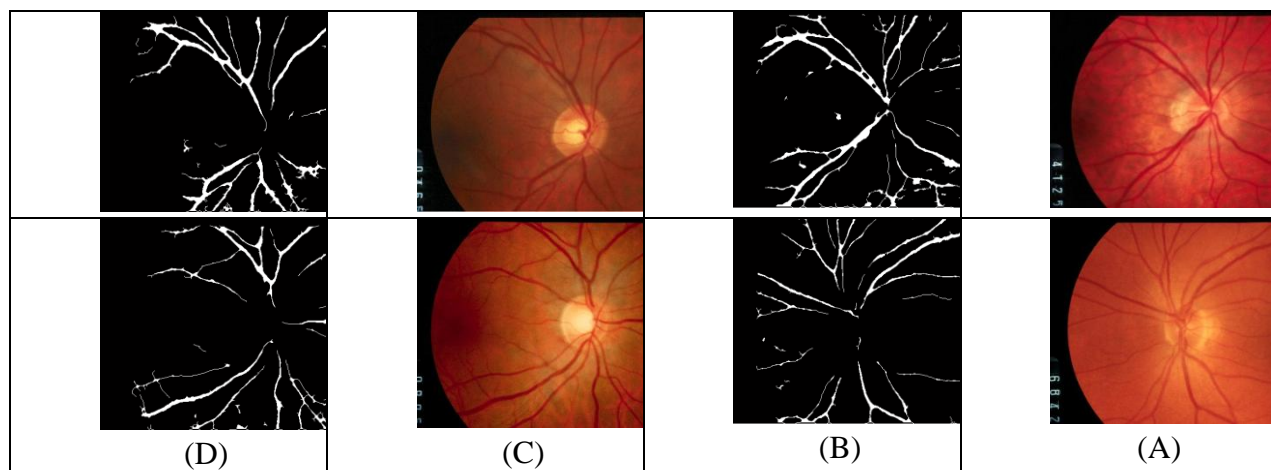


**Figure 16. Results of blood vessels segmentation from retinal images under different conditions**

**(A,C) Original Image (B,D) Blood Vessels Region**

#### 4.4 Segmentation Accuracy:

To judge the segmentation accuracy, we define the segmentation accuracy by equation (11):

$$\text{Segmentation Rate} = \frac{\text{Number of corrected segmented image}}{\text{total database size}} \quad (11)$$

The accuracy of our segmentation algorithm is illustrated in table (1).

**Table 1. Segmentation Rate of Proposed Systems**

Segmented Region	Database	Number of Images	Segmentation Rate
Optic Nerve	DRIVE	100	84%
Optic Nerve	STARE	50	82%
Blood Vessels	DRIVE	100	100%
Blood Vessels	STARE	100	100%

As results show, the proposed algorithm successes in segmenting the retinal images and get the optic nerve and blood vessels. The algorithm also segments the images under different illumination conditions such as darkness and high-brightness.

The proposed algorithm is robustness against different illumination and color conditions and different mage's sources.

#### 4.5 Comparative study:

In the following, there is a comparative study between our study and the others in the same interval of biomedical image processing.

**Table 2. Comparative Study:**

Researcher, Date	Methods	Results		Databases
Sinthanayothin 1988 [9]	Highest average variation	STARE	42.00	STARE & Local
		local	99.10	
Hoover 1998 [14]	Fuzzy convergence	STARE	89.00	STARE & Local
Lalonde 2001 [1]	Hausdorff-based template matching	STARE	71.60	STARE & Local
		local	100.00	
Walter and Klein 2001 [12]	Largest brightest connected object	STARE	58.00	STARE & Local
		local	100.00	
Barrett et al. 2001 [13]	Hough transform as implemented by haar	STARE	59.30	STARE & Local
		local	-	
Osareh et al. 2002 [11]	Averaged optic disc- images	STARE	58.00	STARE & Local
		local	100.00	
Haar 2005 [2]	Resolution pyramid using a simple Haar- based	STARE	70.40	STARE & Local
		local	89.00	
Tobin et al. 2006 [15]	Vasculature-related OD	local	81.00	Local
Abramoff and Niemeijer 2006 [16]	Vasculature related OD properties and a KNN regression	local	99.90	Local
R.ANAND, G.ARAVINTH BABU, K.DEEPA, V.LEKHA 2012 [3]	Active Contour Model Vector Flow model Chan-Vese model	Not Mentioned		Not Mentioned
Arumugam ,Nivedha 2013 [4]	K-means clustering and Independent Component Analysis (ICA)	STARE and DRIVE 40-53 images		94.3% 100%
Deepali A. Godse Dattatraya S. Bormane 2013 [8]	Clustering and computational operation based detection	98.45%		Diaretdb0 (130 images), Diaretdb1 (89 images), Drive (40 images) and local database (194 images)
Josef Hájek, Martin Drahanský,	bifurcations (points where a single	Blood vessels	DRIVE 92,90%	STARE and DRIVE



RadekDrozd2013 [6]	vessel splits into two vessels) in retina		STARE 79,62%	databases
		Optic nerve	STARE:64% DRIVE 85%	
OakarPhyo, AungSoeKhaing 2014 [5]	Mathematical morphology methods such as closing, filling, morphological reconstruction and Otsu algorithm	Not Mentioned		websites and "Eye and ENT General Hospital (Mandalay)
KittipolWisaeng NuulsawatHiransakolwong EkkaratPothiruk 2014 [10]	Morphological method and Otsu's algorithm after the key preprocessing steps, i.e., color normalization, contrast enhancement and noise removal.	STARE	91.35%	STARE & Local
		local	70.61%	
Our approach	Morphological operations, Statistical equations, Histogram-Based illumination correction	Optic Nerve	STARE:80% DRIVE:84%	STARE (50) and DRIVE (100) databases
		Blood Vessels	Both 100%	STARE (100) and DRIVE (100)

## References

1. LALONDE, M, "Fast and robust optic disc detection using pyramidal decomposition and Hausdorff-based template matching", IEEE Trans. Med. Imaging, 2001.
2. HAAR, T. F., "Automatic localization of the optic disc in digital color images of human retinal", Utrecht University, 2005.
3. R.ANAND, G.ARAVINTH BABU, K.DEEPA and V.LEKHA, "SEGMENTATION OF OPTIC DISC INFUNDUS IMAGES", Indian Journal of Computer Science and Engineering, Vol. 3, 2012, pp.230-234.
4. G ARUMNUGAM and S NIVEDHA, "Optic Disc Segmentation Based on Independent Component Analysis and K-Means Clustering", International Journal of Emerging Trends & Technology in Computer Science, vol. 2, 2013, pp.68-73.

5. PHYO, and A KHAING, “*AUTOMATIC DETECTION OF OPTIC DISC AND BLOOD VESSELS FROM RETINAL IMAGES USING IMAGE PROCESSING TECHNIQUES*”, International Journal of Research in Engineering and Technology, Vol. 3, 2014, pp. 300-307.
6. J HAJEK, M DRAHANSKY, and R DROZD, “*Extraction of Retina Features Based on Position of the Blood Vessel Bifurcation*”, Vol. 2, 2013, pp.55-58.
7. RAFAEL C. GONZALEZ , “*Digital Image Processing*”, Prentice Hall, University of Tennessee , New Jersey, 2002.
8. A DEEPALI, and S. BORMANE, “*Automated Localization of Optic Disc in Retinal Images*”, Vol. 4, 2013, pp.65-71.
9. SINTHANAYOTHIN, C., “*Automated localization of the optic disc, fovea and retinal blood vessels from digital color fundus images*”. Br. J. Ophthalmol., 1988, pp: 902-910
10. K WISAENG, N HIRANSAKOLWONG, and E POTHIRUK, “*Automatic Detection of Optic Disc in Digital Retinal Images*”, International Journal of Computer Applications, Vol. 90, 2014, pp.15-20.
11. OSAREH, A., MIRMEHDI, M., THOMAS, B., MARKHAM, R., “*Classification and localization of diabetic-related eye disease*”, Proceeding of the 7th European Conference on Computer Vision Copenhagen, Vision, 2002, pp.502-516.
12. WALTER, T., KLEIN, J. C., “*Segmentation of color fundus images of the human retina: Detection of the optic disc and vascular tree using morphological techniques*”, Proceedings of the 2nd International Symposium on Medical Data Analysis, 2001, pp.282-287.
13. BARRETT, S. F., NAESS, E., MOLVIK, T., “*Employing the hough transform to locate the optic disk*”. Biomed. Sci. Instrum, 2001.
14. HOOVER, A., “*Fuzzy convergence*”, IEEE Xplore Press, Santa Barbara, Proceeding of the Conference Computer Vision and Pattern Recognition”, 1988, pp.716-721.
15. TOBIN, K. W., TOBIN, J. R., CHAUM, E., GOVINDASAMY, V.P., KARNOWSKI, T. P., “*Characterization of the optic disc in retinal imagery using a probabilistic approach*”, Med. Image, 2006, pp. 1088-1097.
16. ABRAMOFF, M. D., NIEMEIJER, M., “*The automatic detection of the optic disc location in retinal images using optic disc location regression*”, Proceeding IEEE Engineering in Medical and Biology Society, 2006, pp.4432-4435.